Journal of the Korean Nuclear Society
Volume 31, Number 6, pp.631~637, December 1999

The Calculation of Neutron Scattering Cross Sections for Silicon Crystal at the Thermal Energies

Young-Sik Cho, Choong-Sup Gil, and Jonghwa Chang
Korea Atomic Energy Research Institute
150 Dukjin-dong, Yusong-gu, Taejon 305-353, Korea
yscho@kaeri.re.kr

(Received August 12, 1999)

Abstract

The module LEAPR of NJOY data processing system has been improved to have the capability of computing the thermal elastic scattering cross sections for silicon, which has a diamond-like structure. Silicon lattice was assumed as an fcc lattice with two atoms at each lattice point.

The calculation formulas for thermal neutron elastic scattering by silicon were introduced and incorporated into LEAPR, and then the scattering cross sections for silicon were computed. The results were compared with experimental data, and they were found to give a good agreement with experimental data.

Key Words : scattering cross section, bragg scattering, silicon, LEAPR, NJOY

1. Introduction

At the thermal energies, the energy transferred by the scattering of a neutron is similar to the kinetic energies of atoms in liquids and solids, and the de Broglie wavelength is comparable to the interatomic distances. Hence, the characteristic motion of atoms and their structures should be taken into account to describe the thermal scattering exactly.

Silicon acts as a very effective thermal neutron filter [1], reducing fast-neutron background. One of its important uses is a fast-neutron attenuator at BNCT (Boron Neutron Capture Therapy) facilities [2]. It is required to determine the characteristics of thermal neutron scattering by silicon to understand the properties of silicon as a filter.

NJOY [3] is widely used as a nuclear data processing tool, and has a built-in module named LEAPR which is able to calculate thermal scattering cross sections for materials of hcp (hexagonal close packed) lattices such as beryllium. This module can be also used to calculate the thermal inelastic scattering cross sections for silicon with only user defined data for phonon frequency spectrum. However, the code can not exactly compute thermal elastic scattering cross sections because the module does not take into account the structure of silicon lattice on which the elastic scattering sensitively depends.

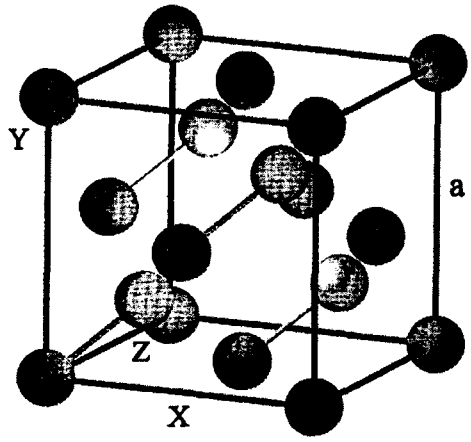

Fig. 1. Diamond-like Structure of Si

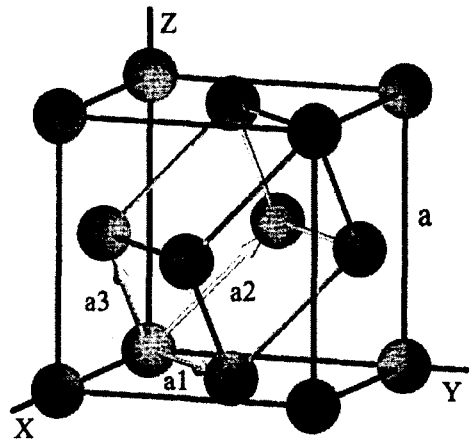

Fig. 2. Primitive Unit Cell of an fcc Structure

In the present article, the module LEAPR of NJOY is improved to have the capability of computing the thermal elastic scattering cross sections for silicon polycrystal, which has a diamond-like lattice structure. The results are compared with experimental data, and they are found to give a good agreement with experimental data.

2. Structure of Silicon Lattice

Silicon has a diamond-like cube structure which consists of two interpenetrating fcc(face-centered cubic) lattices with one being replaced from the other by 1/4 of the principal diagonal of the cube [Fig. 1]. It can be simplified as a single fcc lattice with each lattice point having two identical atoms, one at (0,0,0), and the other at (1/4, 1/4, 1/4).

In case of fcc lattice, primitive lattice vector $\boldsymbol{T}$ can be expressed as:

$$\boldsymbol{T} = u_1\boldsymbol{a}_1 + u_2\boldsymbol{a}_2 + u_3\boldsymbol{a}_3, \tag{1}$$

where u_1 , u_2 and u_3 are integers which can take all possible values including zero, and $\boldsymbol{a}_1$, $\boldsymbol{a}_2$ and $\boldsymbol{a}_3$ are the primitive translation vectors which construct the primitive unit cell, defined as:

$$\begin{aligned} \boldsymbol{a}_1 &= \frac{1}{2}a(\hat{x}+\hat{y}), \\ \boldsymbol{a}_2 &= \frac{1}{2}a(\hat{y}+\hat{z}), \\ \boldsymbol{a}_3 &= \frac{1}{2}a(\hat{z}+\hat{x}), \end{aligned} \tag{2}$$

where $\hat{x}$, $\hat{y}$ and $\hat{z}$ are the unit vectors in a cartesian coordinate system, and a is the length of the cube edge called lattice constant [Fig. 2]. For silicon, the lattice constant a is 5.42 Å [4].

The reciprocal lattice vector is defined as

$$\boldsymbol{\tau} = l_1\boldsymbol{b}_1 + l_2\boldsymbol{b}_2 + l_3\boldsymbol{b}_3 \tag{3}$$

where l_1, l_2 and l_3 are integers which can take all possible values including zero, and $\boldsymbol{b}_1$, $\mathbf{b}_2$ and $\boldsymbol{b}_3$ are primitive translation vectors of reciprocal lattice, defined as:

$$\begin{aligned} \boldsymbol{b}_1 &= 2\pi\frac{\boldsymbol{a}_2\times\boldsymbol{a}_3}{\boldsymbol{a}_1\cdot\boldsymbol{a}_2\times\boldsymbol{a}_3} \\ &= \frac{2\pi}{a}(\hat{x}+\hat{y}-\hat{z}), \\ \boldsymbol{b}_2 &= 2\pi\frac{\boldsymbol{a}_3\times\boldsymbol{a}_1}{\boldsymbol{a}_1\cdot\boldsymbol{a}_2\times\boldsymbol{a}_3} \\ &= \frac{2\pi}{a}(-\hat{x}+\hat{y}+\hat{z}), \\ \boldsymbol{b}_3 &= 2\pi\frac{\boldsymbol{a}_1\times\boldsymbol{a}_2}{\boldsymbol{a}_1\cdot\boldsymbol{a}_2\times\boldsymbol{a}_3} \\ &= \frac{2\pi}{a}(\hat{x}-\hat{y}+\hat{z}), \end{aligned} \tag{4}$$

and it is evident from (2) and (4) that

$$\boldsymbol{a}_i \cdot \boldsymbol{b}_j = 2\pi\delta_{ij} , \quad (5)$$

where the symbol δ_{ij} is the Kronecker delta.

3. Elastic Scattering

Through the thermal elastic scattering by the bound nuclei, the energy of a neutron remains unchanged. This should be distinguished from the elastic scattering by a single particle where the neutron loses energy. The thermal elastic scattering can be divided into two parts: coherent scattering and incoherent scattering. For crystalline solids such as silicon, scattered waves interfere with each other, resulting in so-called Bragg scattering, which is a coherent elastic scattering. The incoherent effect is important for hydrogenous materials and neglected in this work.

3.1. Bragg Scattering

As a consequence of symmetry of crystal lattice, Bragg scattering occurs if

$$\Delta\mathbf{k} = \mathbf{k} - \mathbf{k}' = \tau(l_1, l_2, l_3), \quad (6)$$

where $\Delta\mathbf{k}$ is scattering vector, $\mathbf{k}$ is the wave vector of the incident neutron, and $\mathbf{k}'$ is the wave vector of the scattered neutron.

Since the Bragg scattering is elastic ($|\mathbf{k}| = |\mathbf{k}'|$), it follows from (6) that

$$|\Delta\mathbf{k}| = 2k\sin\theta = |\tau| = \frac{2\pi n}{d} \quad (7a)$$

or

$$2d\sin\theta = n\lambda , \quad (7b)$$

where θ is the Bragg angle between $\mathbf{k}$ and the Bragg planes which are orthogonal to τ. d is the spacing between Bragg planes, and λ is the wavelength of the incident neutron.

Eq. (7b) shows that no Bragg scattering can occur when the wavelength of the incident neutron is larger than twice the largest spacing d_{max} of Bragg planes. When λ reaches $2d_{max}$ ($k=\tau_{min}/2$, where τ_{min} is the smallest length of the reciprocal lattice vector), the first Bragg scattering occurs at the incident angle of 90°. In crystalline solids, there exist many Bragg planes which satisfy Eq. (7b) and the energies corresponding to these critical values ($k_i = \tau_i/2$),

$$E_i = \frac{\hbar^2 k_i^2}{2m} = \frac{\hbar^2 \tau_i^2}{8m} \quad (8)$$

are usually called the Bragg edges. Here m is the mass of a neutron.

3.2. Elastic Cross Section for Silicon

The coherent elastic cross section for a polycrystal [5] is given by

$$\sigma_{coh} = \frac{\pi^2\sigma_c}{nVk^2} \sum_{\tau}^{\tau\le 2k} \frac{1}{\tau} e^{-2W(\tau)} |F(\tau)|^2 , \quad (9)$$

where n is the number of atoms in the primitive unit cell, V is the volume of the primitive unit cell, σ_c is the effective bound coherent scattering cross section for the material, $e^{-2W(\tau)}$ is the Debye-Waller factor, and $F(\tau)$ is the unit cell structure factor. The summation extends over all reciprocal lattice vectors whose magnitudes are not greater than 2k.

At each Bragg edge which satisfies Eq. (8), the coherent scattering cross section shows the sharp Bragg peak, and then decreases proportionally to E^{-1} with increasing neutron energy up to the next Bragg edge. Each Bragg peak arises by reflection of neutrons from a new set of Bragg planes which satisfy Eq. (7b). At energies greater than 0.1 eV, the cross section varies smoothly due to

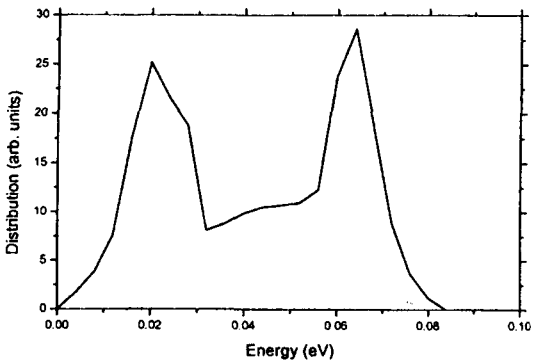

Fig. 3. The Phonon Frequency Spectrum of Si

contribution of so many such planes.

The Debye-Waller factor reflects the influence of the atomic motions on the coherent elastic scattering. As the temperature of the material increases, the Debye-Waller factor decreases due to the increased thermal motions of atoms, reducing the intensity of the Bragg scattering. $W(\tau)$ in the Debye-Waller factor is calculated using the phonon frequency spectrum of the silicon lattice in the module LEAPR. Fig. 3 shows the phonon frequency spectrum used for this work, which is expressed as a function of the phonon energy. This spectrum is that of coarse-grained silicon powders measured by Nesterenko et al.[6]. Average grain size was 100μm, so that this curve can be approximated as representing the phonon spectrum of the bulk of the silicon lattice.

The unit cell structure factor is defined as

$$F(\tau) = \sum_{s=1}^{n} e^{i\tau\cdot\rho_s}, \tag{10}$$

where n is the number of atoms in the primitive unit cell and ρ_s is the positions of atoms in the primitive unit cell. If the crystalline structure is such that only one atom is contained per primitive unit cell, the structure factor is equal to 1. In the case of silicon, there are two atoms in the primitive unit cell at positions (0,0,0), (1/4, 1/4, 1/4), so that

$$\rho_0 = 0, \quad \rho_1 = \frac{a_1 + a_2 + a_3}{4} \tag{11}$$

Thus, using Eq. (3) and Eq. (5), we obtain

$$\begin{aligned} |F(\tau)|^2 &= |\sum_{s=1}^{n} e^{i\tau\cdot\rho_s}|^2 \\ &= |1 + e^{i2\pi(l_1+l_2+l_3)/4}|^2 \\ &= 2 + 2\cos[2\pi(l_1+l_2+l_3)/4]. \end{aligned} \tag{12}$$

For fcc lattice, the volume of the primitive unit cell is

$$V = a_1 \cdot a_2 \times a_3 = \frac{a^3}{4} \tag{13}$$

and, from Eq. (3) and Eq.(4), τ is given by

$$\begin{aligned} \tau &= (\frac{2\pi}{a})\sqrt{(l_1-l_2+l_3)^2+(l_1+l_2-l_3)^2+(-l_1+l_2+l_3)^2} \\ &= (\frac{2\pi}{a})\sqrt{3l_1^2+3l_2^2+3l_3^2-2l_1l_2-2l_2l_3-2l_3l_1}. \end{aligned} \tag{14}$$

4. Inelastic Scattering for Silicon

Inelastic scattering includes both the coherent and incoherent contributions. The numerical calculation of such scattering is considerably simplified by two approximations: the incoherent approximation and the Gaussian approximation. In the incoherent approximation, the interference effect of inelastic scattering is neglected. The approximation is valid for neutrons with energies greater than about 0.001 eV where the interference effect is practically negligible. In the Gaussian approximation, the intermediate scattering function is represented as a Gaussian function of the scattering vector. The intermediate scattering function is such a function that describes the thermal scattering.

With these approximations, the inelastic scattering cross sections for thermal neutrons can

Table 1. The Physical Constants Used for the Calculations

Coherent bound scattering cross section	2.16 barns [7]
Weight ratio to neutron	27.844
Free atom cross section	2.042 barns

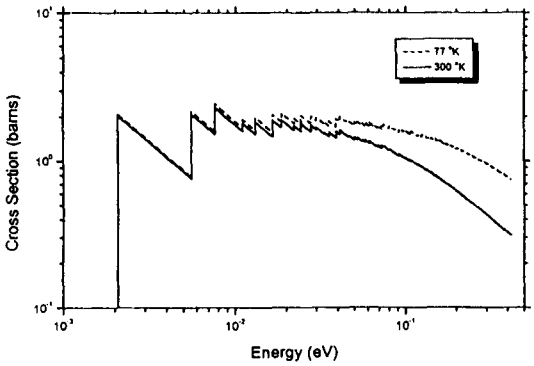

Fig. 4. The Elastic Cross Sections for Si

be obtained from the exact shape of the phonon frequency distribution. The module LEAPR needs as an input the phonon frequency spectrum of the material being considered. We used the experimentally determined phonon frequency spectrum of the silicon crystal [6].

5. Calculations and the Results

The formulas for the thermal neutron elastic scattering by silicon, which were introduced in section 3.2, are incorporated into the module LEAPR of NJOY. The module is used to calculate the thermal elastic scattering cross sections for silicon polycrystal. This method can be also applied for other materials which have diamond-like structures such as germanium. The effect of inelastic scattering is taken into account by using the phonon frequency spectrum of the silicon crystal. The calculations were performed

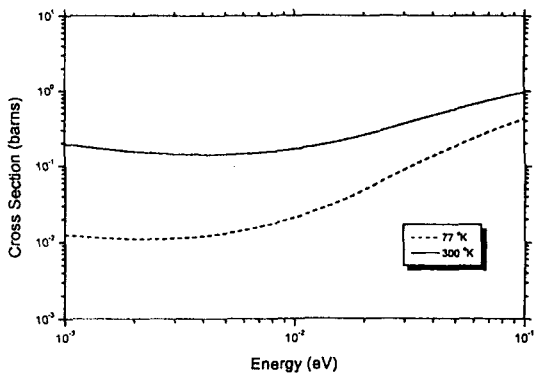

Fig. 5. The Inelastic Cross Sections for Si

at 77°K and 300°K. The physical constants used for the calculations are shown in Table 1.

The computed coherent elastic scattering cross sections showing the Bragg edges and peaks are graphed in Fig. 4. Notice that the cross section is zero for energies below 2.08 meV, which is called the Bragg cut-off. Each Bragg edge corresponds to the value obtained from Eq. (8). The Bragg peaks represent a positive interference of neutron waves scattered from a new set of Bragg planes in silicon lattice. The peaks are a little lower at the higher temperature because of the increased thermal motion of silicon atoms.

In Figs. 5 and 6, inelastic cross sections and total scattering cross sections are shown. Notice that the computed inelastic cross sections are larger at the higher temperature due to the increased thermal motion of atoms.

In Fig. 7, the total cross sections computed at 300°K are compared with the experimental data. The experimental data were given as the total cross sections, so for comparison, the theoretical total cross sections were obtained by adding the silicon capture cross sections from ENDF/B-VI [8] to the total scattering cross sections calculated in this work. The experimental data were

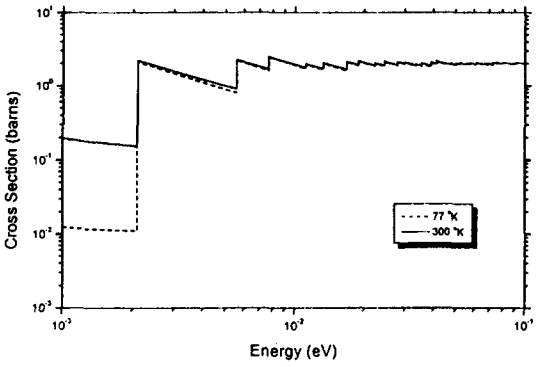

Fig. 6. The Total Scattering Cross Sections for Si

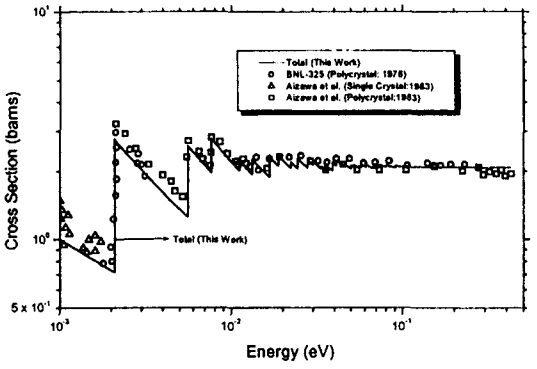

Fig. 7. The Total Cross Sections at 300° K for Si

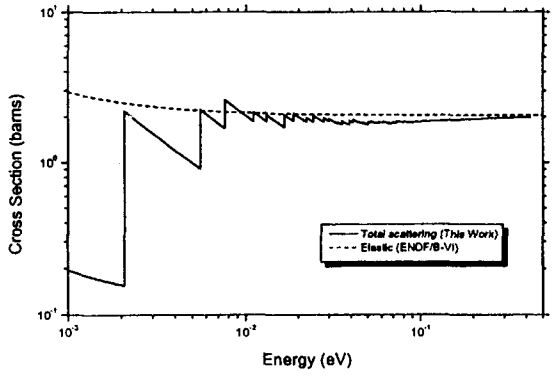

Fig. 8. The Total Scattering Cross Sections at 300° K for Si

obtained from BNL-325 [9] and the work of Aizawa and Matsumoto [10], and these experiments were performed at room temperature. It is evident from the figure that the calculated total cross sections give a good agreement with the measured data. The agreement for the Bragg edges is very good.

In Fig. 8, the scattering cross sections calculated at 300 °K are compared with the elastic cross section data from ENDF/B-VI. The cross section data from ENDF/B-VI are those for a single free nucleus. The elastic cross sections obtained from ENDF/B-VI are larger than the calculated values at lower energies but tend to coincide with them at higher energies.

6. Conclusions

The attempt to calculate the thermal neutron scattering cross sections for the silicon crystal was made in this article. Silicon lattice was assumed as an fcc lattice with two atoms at each lattice point. The calculation formulas for thermal neutron elastic scattering cross sections for the silicon were introduced and incorporated into the module LEAPR of NJOY, and then the scattering cross sections were computed. The inelastic scattering cross sections were calculated using the experimentally determined phonon frequency spectrum for silicon. This improved module can be also used to obtain the scattering cross sections for the other materials which have diamond-like structures such as germanium by changing the lattice constants and the coherent bound scattering cross section in the source code.

The calculated results were compared with the experimental data. The results were found to give a good agreement with the experimental data. Bragg edges and peaks shown in the calculated coherent elastic cross sections agreed well with those in the experimental data.

Acknowledgement

This work is performed under the auspices of the Korean Ministry of Science and Technology.

References

1. R. M. Brugger and W. Yelon, "Use of Single Crystal Silicon as a Thermal Neutron Filter," Proc. Conf. on Neutron Scattering, Tennessee, USA, Jun 6, p. 1117-1122 (1976).
2. B. J. Jun and B. C. Lee, "Design of a BNCT facility at HANARO," Proc. 6th Meet. IGORR, Taejon, Korea, April 29 - May 1, p. 245-250, Korea Atomic Energy Research Institute (1998).
3. R. E. MacFarlane and D. W. Muir, "The NJOY Data Processing System Version 91," LA-12740-M (Oct. 1994).
4. S. Flügge, "Handbuch der Physik," Vol. VII/1 (1955).
5. D. E. Parks, M. S. Nelkin, J. R. Beyster, and N. F. Wikner, Slow Neutron Scattering and Thermalization, W. A. Benjamin, Inc., New York (1970).
6. B. A. Nesterenko, B. I. Gorbachev, V. A. Zrazhevskii, P. G. Ivanitskii, V. T. Krotenko, M. V. Pasechnik, and O. V. Snitko, "Phonon spectrum of the silicon lattice," Sov. Phys. Solid State, **16**, 2284 (May 1975).
7. Stephen W. Lovesey, Theory of Neutron Scattering from Condensed Matter: Vol. 1, p.17, Oxford Science Publications, New York, (1987).
8. P. F. Rose, "Cross Section Evaluation Working Group, ENDF-VI Summary Documentation," BNL-NCS-17541 (ENDF-201) (1991).
9. D. I. Garber and R. R. Kinsey, BNL-325, 3rd ed. (1976).
10. O. Aizawa and T. Matsumoto, "Total Neutron Cross Sections of Magnesium, Aluminum, Silicon, Zirconim, Niobium and Molybdenum in Energy Range from 0.001 to 0.3 eV," J. Nucl. Sci. Technol.(Tokyo, Japan), **20**, 713 (September 1983).